

Bond-disordered spin systems: Theory and application to doped high- T_c compounds

Frank Krüger and Stefan Scheidl

Institut für Theoretische Physik, Universität zu Köln, Zùlpicher Strasse 77, D-50937 Köln, Germany

(Received 9 October 2001; revised manuscript received 29 January 2002; published 22 May 2002)

We examine the stability of magnetic order in a classical Heisenberg model with quenched random exchange couplings. This system represents the spin degrees of freedom in high- T_c compounds with immobile dopants. Starting from a replica representation of the nonlinear- σ model, we perform a renormalization-group analysis. The importance of cumulants of the disorder distribution to arbitrarily high orders necessitates a functional renormalization scheme. From the renormalization flow equations we determine the magnetic correlation length numerically as a function of the impurity concentration and temperature. From our analysis it follows that two-dimensional layers can be magnetically ordered for arbitrarily strong but sufficiently diluted defects. We further consider the dimensional crossover in a stack of weakly coupled layers. The resulting phase diagram is compared with experimental data for $\text{La}_{2-x}\text{Sr}_x\text{CuO}_4$.

DOI: 10.1103/PhysRevB.65.224502

PACS number(s): 75.10.Nr, 74.72.-h, 75.50.Ee

I. INTRODUCTION

Although the interest in disordered spin systems reaches back several decades (for a review, see, e.g., Ref. 1), interest has strongly revived in recent years as a result of the recognition that high- T_c compounds exhibit phases with antiferromagnetic (AFM) order, spin-glass order, or stripe order in certain ranges of temperature and doping. A prominent example for such materials is $\text{La}_{2-x}\text{Sr}_x\text{CuO}_4$, in which every Cu atom carries a spin $\frac{1}{2}$ (for an overview on this material, see, e.g., Ref. 2).

In these materials, the spins are located in weakly coupled layers. Within each layer, the spins constitute a square lattice with antiferromagnetic exchange coupling between nearest neighbors.³ In the undoped system, these spins can be represented to a good approximation by a classical two-dimensional model since quantum fluctuations lead to a merely quantitative renormalization of the classical parameters.⁴ Although a weak coupling between the layers and a weak easy-plane anisotropy are present in these materials (both are about five orders-of-magnitude smaller than the isotropic intraplane exchange⁵), they become relevant only on relatively large scales. Thus, on the finite length scales of experimental relevance, the spins can be described in a first approximation by a classical Heisenberg antiferromagnet in two dimensions.

Doping induces holes in the layers, which can lead to quenched frustration of the exchange couplings. Frustration can occur when the holes are localized individually^{6,7} as well as when they condense into a topologically defective array of stripes which act as antiphase domain walls for the AFM order.⁸⁻¹⁰ Both cases can be represented by an effective bond-disordered Heisenberg model. Such a system is expected to display generic spin-glass behavior, as is observed in experiments beyond a critical doping.¹¹

On the theoretical side, Heisenberg spin glasses are much less understood than Ising spin glasses. While it is well established for the pure two-dimensional (2D) system that the magnetic correlation length ξ decays exponentially with increasing temperature,¹² the dependence of ξ on disorder is controversial. At $T=0$ it is not clear whether ξ is finite for

every small but finite concentration of defect bonds^{13,14,15} or whether ξ is infinite up to a critical concentration even for strong defects.¹⁶ Concerning the temperature dependence of ξ , there is no consensus as to whether it is reentrant¹⁴ or not.¹⁵ To readdress these unsettled issues, we develop a theoretical approach for bond-disordered spin glasses which complements previous approaches. In particular, we calculate the correlation length and compare our results to the results of previous theoretical approaches and experiments on high- T_c compounds.

The outline of the paper is as follows. In Sec. II we establish the model and briefly review the mechanism by which holes generate magnetic textures that provide the nucleus for a reduction of magnetic order. Based on this mechanism, we further examine our motivation as to why it is desirable to develop an alternative to previous theoretical approaches. In Sec. III, we derive the functional renormalization-group equations. These flow equations are evaluated numerically and our results for the magnetic correlation length are compared to experimental data in Sec. IV, where we also consider the dimensional crossover from 2D to 3D behavior. We conclude with a discussion of our results in Sec. V.

II. MODEL

In a system with sparse substitutional doping, the dopants can be considered as randomly distributed with negligible correlations and quenched over a wide temperature range. In doped Mott insulators, the effect of the dopants is twofold: they induce holes in the cuprate planes and at the same time they provide a random potential that localizes these holes at sufficiently low temperatures. Therefore, they are commonly assumed to be localized on the oxygen atoms between neighboring copper atoms.^{6,17,7}

A simple argument suggests that such a hole transmutes the antiferromagnetic superexchange coupling between the neighboring copper spins into a ferromagnetic one. Thereby frustration is induced in the spin system.⁶ The irrelevance of quantum fluctuations of the spins in the pure system⁴ (in the sense that they lead only to a quantitative renormalization of

classical parameters such as the spin stiffness) suggests that they may be neglected in a good approximation also for small doping.¹⁸

A. Definition

Starting from a classical description of the antiferromagnetism, we may examine an equivalent model where all spins of one bipartite sublattice are flipped and the sign of all exchange couplings is reversed,¹⁹ i.e., we now consider the coupling of the undoped system to be ferromagnetic and the defect couplings to be antiferromagnetic. We base our analysis on the Hamiltonian

$$H = \frac{1}{2} \sum_{\mathbf{r}, i} J_i(\mathbf{r}) [\nabla_i \vec{S}(\mathbf{r})]^2 \quad (1)$$

for spins on a (hyper)cubic lattice in d dimensions (a single layer is described by $d=2$). Spins are treated as classical N -component vectors of unit length, $\vec{S}^2(\mathbf{r}) = 1$. A spin at site \mathbf{r} is coupled to its nearest neighbor in the direction $i = 1, \dots, d$ via the exchange coupling $J_i(\mathbf{r})$. We define $\nabla_i \vec{S}(\mathbf{r}) := \vec{S}(\mathbf{r} + \mathbf{a}_i) - \vec{S}(\mathbf{r})$ for a basis vector \mathbf{a}_i . The global symmetry $O(N)$ of spin rotations is preserved for arbitrarily disordered exchange couplings.

It is convenient to rewrite the exchange coupling as

$$J_i(\mathbf{r}) = [1 - \Delta_i(\mathbf{r})]J \quad (2)$$

with the value $J > 0$ of the pure system and the quenched random variable $\Delta_i(\mathbf{r})$. Frustration effects emerge for $\Delta_i(\mathbf{r}) > 1$, when a ferromagnetic bond becomes antiferromagnetic. To further specify the nature of the disorder, we assume a bimodal distribution of the exchange couplings,

$$\Delta_i(\mathbf{r}) = \begin{cases} \Delta & \text{with probability } p, \\ 0 & \text{with probability } 1 - p. \end{cases} \quad (3)$$

For square lattices such as in $\text{La}_{2-x}\text{Sr}_x\text{CuO}_4$, the concentration x is related to this probability by $x = 2p$. Correlations between different bonds are assumed to be absent.

B. Single defects

Before we address the magnetic order in the presence of a finite concentration of defects, it is instructive to recall briefly the physics of a *single* defect for $N \geq 2$. While the ground state of the pure system is collinear (all spins are strictly parallel), it is canted (i.e., no longer collinear) for a single defect beyond a certain critical strength Δ_{single} .^{13,20,21} The threshold $\Delta_{\text{single}} = d$ value can be obtained from a spin-wave calculation²² (see also Appendix B). The ground state for a single defect with $\Delta > \Delta_{\text{single}}$ remains *planar* for all $N \geq 2$, i.e., apart from a global rotation, the defect texture for Heisenberg spins ($N=3$) is identical to the texture for XY spins ($N=2$). Far away from the defect bond, the texture is described by the solution of the Laplace equation¹³

$$\nabla^2 \vec{S}(\mathbf{r}) = 0 \quad (4)$$

and the spins approach a collinear configuration, $\vec{S}(\mathbf{r}) \rightarrow \vec{S}_0$ for $r \rightarrow \infty$. To be specific, we discuss a defect bond located at $\mathbf{r} = 0$ and oriented in direction \mathbf{a} . It acts as a source of a dipolar distortion with a moment $\vec{\mu}$ perpendicular to \vec{S}_0 . For $d=2$, in particular,

$$\vec{S}(\mathbf{r}) - \vec{S}_0 \approx \frac{\vec{\mu}}{2\pi} \frac{\mathbf{a} \cdot \mathbf{r}}{r^2}. \quad (5)$$

The amplitude of the dipole moment is determined by the nonlinearity of the model, which may be considered as interaction between spin waves. The magnetic textures of several defect bonds are subject to a dipolar interaction at large distances.^{13,20} The effects of a finite density of defects are nontrivial because of the frustrated long-range interaction between the dipoles. In the presence of more than two defects, the interaction among the dipoles typically becomes frustrated. Then the ground state is no longer planar for $N > 2$.

C. Finite defect concentration

Depending on the relative position of several defect bonds in a cluster, the generated texture may have a dipolar or higher-order multipolar structure. In contrast to electrostatics, the multipolar moments of defect textures are not additive since the spins act as a nonlinear medium for the dipoles, giving rise to many-body interactions. In particular, clusters of defects can lead to canting already for defect-bond strengths *below* Δ_{single} , i.e., in clusters of defects the threshold strength of the defect bonds is reduced. The threshold values of some specific bond configurations in the XY model are given in Refs. 22 and 23 (see in particular Table I in the latter). In general, threshold values in the XY system are upper bounds for the thresholds in a Heisenberg system since with increasing N the spins have a larger space of canted states which they may explore to minimize energy.

Thus, as soon as the defects are antiferromagnetic ($\Delta > 1$) they can induce canted textures due to the presence of arbitrarily large clusters.^{13,22–24} Hence the ground state will be canted for *every* $p > 0$ and $\Delta > 1$ (assuming that the defect distribution has no pathological spatial correlations). Therefore one may expect a system with a certain density of weak defects $1 < \Delta < \Delta_{\text{single}}$ to be qualitatively equivalent to a system with a (possibly much) smaller concentration of strong defects $\Delta > \Delta_{\text{single}}$.

The presence of canting certainly implies a reduction of magnetization. However, one cannot draw direct conclusions about the range of magnetic order. For a sufficiently high density of strong defects, one certainly has short-range order. For defects of a weaker strength or a lower concentration, one can have also quasi-long-range order (as in an XY model with quenched and uncorrelated dipoles;^{23,25} see also Ref. 26 for an XY model with thermal dipoles at a fixed density). A phase with true long-range order is also possible but unlikely since it would require a highly ordered dipole configuration.

It is instructive to recall a “duality” relation²⁷ in the (p, Δ) parameter space, since in a mixture of ferromagnetic and antiferromagnetic bonds there are two ways to declare

one type as “regular” bond and the other type as “defect” bond (see Appendix A). This duality implies a relation

$$\Delta_{\text{AFM}}(p) = \frac{\Delta_{\text{FM}}(1-p)}{\Delta_{\text{FM}}(1-p) - 1} \quad (6)$$

between boundary lines $\Delta_{\text{FM}}(p)$ and $\Delta_{\text{AFM}}(p)$ limiting regions with ferromagnetic order (for $\Delta < \Delta_{\text{FM}}$) and antiferromagnetic order (for $\Delta > \Delta_{\text{AFM}}$) in the (p, Δ) plane. Since the duality relation maps the region $p\Delta > 1$ onto $p\Delta < 1$ it is sufficient to examine the latter region.

To perform first qualitative estimates, one may consider the disorder-averaged exchange coupling, which is

$$\overline{J_i(\mathbf{r})} = (1-p\Delta)J \quad (7)$$

for the bimodal distribution (3). Thus, there is a tendency towards the formation of ferromagnetic order for $p\Delta < 1$ (where $\bar{J} > 0$) and a tendency towards antiferromagnetic order for $p\Delta > 1$ (where $\bar{J} < 0$). Certainly, the presence of order requires more than such a tendency. A further minimum requirement should be that the relative fluctuations

$$\sigma^2 := \frac{\overline{J_i^2(\mathbf{r})} - \overline{J_i(\mathbf{r})}^2}{\overline{J_i(\mathbf{r})}^2} = \frac{p(1-p)\Delta^2}{(1-p\Delta)^2} \quad (8)$$

of the exchange couplings must be small. Since $\Delta > 1$ and $p\Delta < 1$ in the range of interest, $\sigma^2 \ll 1$ requires $p\Delta^2 \ll 1$. A very crude estimate of the boundary from $\sigma \approx 1$ suggests

$$\Delta_{\text{FM}}(p) \approx p^{-1/2}. \quad (9)$$

For the special case $\Delta = 1$, the defect bonds have a vanishing exchange coupling and the system is bond diluted. The presence of magnetic order (in the sense of a finite magnetization) then requires that a finite fraction of spins is connected by regular bonds. This is the case below the percolation transition, i.e., for $p < \frac{1}{2}$ in $d=2$.²⁸ Therefore one expects $\Delta_{\text{FM}}(p) = 1$ for $p \geq \frac{1}{2}$.

D. Previous work

To our best knowledge, there are only a few approaches in the literature aimed at a more sophisticated analysis, which we briefly summarize in order to highlight our motivation to reconsider this problem in an alternative way. First, the coherent-potential approximation (CPA) provides a simple self-consistent approach to determine an effective spin stiffness for the random system. For $N=2$, the CPA yields²⁹ a transition line $\Delta_{\text{FM}}^{\text{CPA}}(p)$ smoothly interpolating between $\Delta_{\text{FM}}^{\text{CPA}}(0) = d$ (reflecting the canting threshold for individual defect bonds) and $\Delta_{\text{FM}}^{\text{CPA}}(p) = 1$ for $p \geq \frac{1}{2}$ in $d=2$ and for $p \geq \frac{2}{3}$ in $d=3$. In $d=2$, the location of the percolation transition is captured exactly. This has to be considered as a fortunate coincidence which is absent in $d=3$, where the location is found only approximately.²⁹ In the limit $N \rightarrow \infty$ the CPA yields that the stability of order requires $\sigma^2 < 1$,¹⁶ which results in $\Delta_{\text{FM}}^{\text{CPA}}(p) \approx p^{-1/2}$ for small p in agreement with the naive estimate (9).

Unfortunately, the interpretation of the CPA is somewhat ambiguous.³⁰ According to its construction, the CPA replaces the disordered system by a ferromagnetic one with a homogeneous effective exchange constant. The strength of this effective coupling is determined from a self-consistency condition that considers the fluctuations of a single bond. Thus, the CPA misses effects of clusters of defect bonds. The putative transition line is defined as the border line up to which self-consistent solutions exist. *A priori*, this border line can be interpreted in two ways: either as the onset of the canting instability or as the onset of short-range magnetic order. Therefore, the CPA can be only of qualitative use.

To gain insight into the nature of the ground state, Gawiec and Gempel^{23,27} (GG) performed numerical studies of the XY model in $d=2$. Their data suggest a transition line $\Delta_{\text{FM}}^{\text{GG}}(p)$ between a phase with quasi-long-range order and short-range order. It starts from at the canting instability $\Delta_{\text{FM}}^{\text{GG}}(0) = \Delta_{\text{single}} = 2$ and follows $\Delta_{\text{FM}}^{\text{GG}}(p) = 1$ beyond the percolation transition. Thus, the data suggest short-range order for an *arbitrarily small* concentration of defects of a strength exceeding the canting instability of single defects in agreement with the CPA. However, as stated in Ref. 23, the question of whether one can have order for $\Delta > \Delta_{\text{single}}$ at sufficiently small p remains far from settled due to finite-size effects.

For the Heisenberg model with the bimodal bond distribution, to our best knowledge, there are only very few numerical studies. For the special case of two dimensions and $\Delta = \Delta_{\text{single}} = 2$, Nonomura and Ozeki³¹ postulated order for $p \leq 0.11$ from an exact-diagonalization method for $S = \frac{1}{2}$ quantum spins. This implies an even larger stability of the classical model, and in particular $\Delta_{\text{FM}}(0) > 2$. However, their conclusion has to be considered with care because of finite-size effects.

Previous analytic approaches^{14,15} are implicitly restricted to defect-bond strengths exceeding the canting threshold, $\Delta \gg \Delta_{\text{single}}$. The spin system with random bonds is *replaced* by a spin system with homogeneous bonds coupled to an additional canting field that also generates dipolar spin textures. In order to shed some light on the quality of this replacement, we perform a Hubbard-Stratonovich transformation introducing an auxiliary bivectorial field \vec{f}_i via

$$\exp(-H[\vec{S}]/T) = \int \mathcal{D}\{\vec{f}\} \exp(-\tilde{H}[\vec{S}, \vec{f}]/T), \quad (10a)$$

with

$$\tilde{H}[\vec{S}, \vec{f}] = J \sum_{\mathbf{r}, i} \left\{ \frac{1}{2} [\nabla_i \vec{S}(\mathbf{r})]^2 - \vec{f}_i(\mathbf{r}) \cdot \nabla_i \vec{S}(\mathbf{r}) + \frac{1}{2\Delta_i(\mathbf{r})} \vec{f}_i^2(\mathbf{r}) \right\}. \quad (10b)$$

In this representation, \vec{S} and \vec{f}_i are thermally fluctuating variables, \vec{S} with spherical constraint, \vec{f}_i unconstrained. In the Hamiltonian (10b) of the transformed system, the spins interact directly via the homogeneous exchange coupling J . In addition, they couple also to the canting field \vec{f}_i . It is precisely such a coupling that was considered in Refs. 14 and 15.

The Hubbard-Stratonovich transformation—which yields an exact representation of the original model (1)—shows that the field \vec{f}_i has a *local* self-interaction potential

$$V_{ij}(\mathbf{r}, \mathbf{r}') = \delta_{ij} \delta_{\mathbf{r}, \mathbf{r}'} J / \Delta_i(\mathbf{r}). \quad (11)$$

On regular bonds with $\Delta_i(\mathbf{r})=0$, $\vec{f}_i(\mathbf{r})$ is suppressed. On defect bonds with $\Delta_i(\mathbf{r})>0$, $\vec{f}_i(\mathbf{r})$ has finite fluctuations. For $\nabla_i \vec{S}(\mathbf{r})=0$ one would have

$$\langle f_i^a(\mathbf{r}) f_j^b(\mathbf{r}') \rangle = \delta_{ij}^ab \delta_{\mathbf{r}, \mathbf{r}'} \frac{T}{J} \Delta_i(\mathbf{r}). \quad (12)$$

However, it is crucial to retain the full correlations between the fluctuations of \vec{S} and \vec{f}_i . The spin-wave saddle-point equation

$$\nabla_i \vec{S}(\mathbf{r}) = \vec{f}_i(\mathbf{r}) \quad (13)$$

immediately shows that \vec{f}_i induces a canting of the spin field. If $\vec{f}_i(\mathbf{r})$ is considered as fixed and nonvanishing only on a single bond, it induces a dipolar spin texture. It is important to notice that the original spin rotation symmetry of Hamiltonian (1) is preserved in the transformed model (10b) only if \vec{f}_i is rotated simultaneously with \vec{S} .

Instead of solving the full problem of two fluctuating fields, Refs. 14 and 15 proceed with additional assumptions about the nature of \vec{f}_i . Glazman and Ioselevich¹⁴ (GI) consider a Hamiltonian, where $\vec{f}_i(\mathbf{r})$ has a *fixed length* on the defect bonds. Only the orientation of $\vec{f}_i(\mathbf{r})$ is considered as a thermal degree of freedom. Thereby the rotation symmetry is preserved. However, fixing the length of $\vec{f}_i(\mathbf{r})$ contradicts Eq. (12), which shows that the magnitude of $\vec{f}_i(\mathbf{r})$ is a thermally fluctuating quantity that vanishes in the limit of zero temperature. This means that in the approach of GI the strength of disorder is *overestimated* at low temperatures. This may be a reason that explains why GI find a reentrant temperature dependence of ξ .

On the other hand, Cherepanov *et al.*¹⁵ consider \vec{f}_i as a *quenched* field with Gaussian correlations. This is in contradiction to the annealed nature of \vec{f}_i as is revealed by the transformed model (10). In addition, spin rotation symmetry is explicitly broken. This treatment is based on the assumption that the spin textures freeze at low temperatures. However, a spontaneous breaking of this symmetry in $d \leq 2$ is ruled out by the Mermin-Wagner theorem.³² Thus, one may worry that disorder effects may be *overestimated* in this approach. Possibly, the artificial symmetry breaking is related to the spurious generation of random fields in a replica treatment as found by Cherepanov *et al.*¹⁵

III. RENORMALIZATION-GROUP ANALYSIS

Although the Hubbard-Stratonovich transformation was useful to relate previous work to the original model, the introduction of \vec{f} is accompanied with additional difficulties. Therefore we choose to continue to work with the original

model where the field \vec{f} is integrated out. Before we perform a renormalization-group (RG) analysis, we use the standard replica trick to treat disorder.

A. Replica representation

After n -fold replication the Hamiltonian reads

$$H^{(n)} = \frac{1}{2} \sum_{\mathbf{r}, i} [1 - \Delta_i(\mathbf{r})] J \psi_i(\mathbf{r}) \quad (14a)$$

with the abbreviation

$$\psi_i(\mathbf{r}) := \sum_{\alpha=1}^n [\nabla_i \vec{S}^\alpha(\mathbf{r})]^2. \quad (14b)$$

(Upper Greek indices label replicas.) Since we assume that the probability distribution of $\Delta_i(\mathbf{r})$ is uncorrelated and identical for all bonds, disorder averaging leads to the local and translation symmetric Hamiltonian (\mathcal{H} includes the factor $1/T$)

$$\mathcal{H} = \sum_{\mathbf{r}, i} \left\{ \frac{1}{2} K \psi_i(\mathbf{r}) - R(\psi_i(\mathbf{r})) \right\}. \quad (15)$$

The cumulant function R is specified by

$$R(\psi_i(\mathbf{r})) := \ln \exp[\overline{\Delta_i(\mathbf{r}) K \psi_i(\mathbf{r}) / 2}] \quad (16)$$

and depends implicitly on $K := J/T$. For the special case of bimodal disorder (3),

$$R(\psi) = \ln[1 - p + p e^{\Delta K \psi / 2}] \quad (17a)$$

$$\approx \begin{cases} \frac{1}{2} p \Delta K \psi & \text{for } \Delta K \psi \rightarrow 0, \\ \frac{1}{2} \Delta K \psi + \ln p & \text{for } \Delta K \psi \rightarrow \infty. \end{cases} \quad (17b)$$

Note that naturally $R(\psi)=0$ in the absence of disorder (for $p=0$ or $\Delta=0$) and that $R(\psi)=\frac{1}{2}\Delta K \psi$ for $p=1$, which amounts to an unfrustrated dual model with a corresponding stiffness $(1-\Delta)J$. In the general case, $R(\psi)$ is a nonlinear function which has linear asymptotics for small and large arguments, cf. Eqs. (17).

Remarkably, the energy depends on ψ only through the combination

$$h(\psi) := K \psi - 2R(\psi). \quad (18)$$

A priori, it is not clear whether spin fluctuations are governed by the behavior of $h(\psi)$ at large ψ or at small ψ .

The stability of the ferromagnetic state with respect to large-scale spin-wave deformations depends on $h(\psi)$ at small ψ and requires $h'(0)>0$, i.e., $p\Delta < 1$. (For $p\Delta > 1$ the dual antiferromagnetic ground state is locally stable.) This condition is equivalent to the requirement that the average exchange coupling (7) should remain ferromagnetic.

While the effective stiffness is defined from the slope of the function $h(\psi)$ at $\psi=0$, its behavior $h(\psi) \sim (1-\Delta)K\psi$

for $\psi \rightarrow \infty$ (which is equivalent to $T \rightarrow 0$) reflects the presence of frustration. For $\Delta < 1$ — i.e., in the *absence* of frustration— $h(\psi)$ is positive for all ψ and fluctuations can renormalize the stiffness to a smaller but positive value. For $\Delta > 1$ —i.e., in the *presence* of frustration— $h(\psi)$ is negative at large ψ and fluctuations can renormalize the stiffness to zero, signaling the destruction of magnetic order.

In the replica representation, the canting instability for a *single* defect can be retrieved easily. To this end, we consider the case in which a single *particular* bond is populated by a hole with probability p . Then, the replica Hamiltonian is similar to Eq. (15) with the modification that one has to keep the cumulant function (17) only on the particular bond and switch it off on all other bonds. In the limit $T \rightarrow 0$ (considering the statistical weight for fixed n and a fixed but arbitrary spin configuration), the replicas decouple since $R(\psi) \approx \frac{1}{2} \Delta K \psi + \ln p$. The exchange coupling of the defect bond within each replica is $(1 - \Delta)J$ independent of p . Thus, canting occurs in the case $p < 1$ for $\Delta > \Delta_{\text{single}}$ as in the case $p = 1$. While the threshold is independent of p , the disorder-averaged dipole moment depends on p . Since ψ becomes arbitrarily small slightly above the canting threshold, this dipole moment cannot be calculated from the large- ψ limit of h .

Therefore in general it is important to retain the *global* functional form of $h(\psi)$ [or, equivalently, $R(\psi)$]. An approximation of this function by a Taylor series near $\psi = 0$ would amount to an expansion in cumulants of the defect distribution. The relevance of $R(\psi)$ for large ψ shows that one could miss essential physics by dropping high-order cumulants and—in particular—using a Gaussian distribution for Δ . Even worse, the function $R(\psi)$ is *nonanalytic*, i.e., its behavior at large ψ is outside the radius of convergence of a cumulant expansion.

B. Flow equations

In order to address the question of magnetic order in the presence of general fluctuations of ψ , we generalize the renormalization-group analysis of Polyakov¹² to the replicated model. Instead of working with the function $h(\psi)$, it is more physical to use an effective bare stiffness and an effective cumulant function defined by

$$K_0 := K - 2R'(0) = (1 - p\Delta)K, \quad (19a)$$

$$R_0(\psi) := R(\psi) - \psi R'(0) = R(\psi) - \frac{1}{2} p \Delta K \psi \quad (19b)$$

to remove the linear contribution of R , which represents a trivial renormalization of the stiffness. The replacement of the original quantities by the effective ones leaves the energy (15) invariant since $K\psi - 2R(\psi) = K_0\psi - 2R_0(\psi)$.

Following Polyakov's analysis of the pure system,¹² we renormalize the model by a momentum-shell integration. So far, the Hamiltonian (15) was written in a way to explicitly retain the lattice of the spin sites. We choose the lattice spacing as the unit of length and go over to a continuum representation by smoothly interpolating the field $\vec{S}(\mathbf{r})$ between

the lattice sites [preserving the normalization $\vec{S}^2(\mathbf{r}) = 1$ everywhere]. In this limit, partial spatial derivatives replace the differences in $\psi_i(\mathbf{r}) = \sum_{\alpha=1}^n [\partial_i \vec{S}^\alpha(\mathbf{r})]^2$ and

$$\mathcal{H} = \int d^d r \sum_i \left\{ \frac{1}{2} K \psi_i(\mathbf{r}) - R(\psi_i(\mathbf{r})) \right\}. \quad (20)$$

The replacement of differences by partial derivatives and of the sum by an integral should be a reasonably good approximation, i.e., the replacement of ψ should lead to small relative errors compared to unity for an *arbitrary* spin configuration (even with inhomogeneities on the scale of the lattice spacing). A small relative error in ψ is equivalent to a small relative misrepresentation of J and/or Δ since these quantities enter the Hamiltonian only as a product with ψ . We further use the approximate replacement of the cubic Brillouin zone by a spherical one. Thus, to preserve the volume of the Brillouin zone, its radius Λ has to be fixed by $\Lambda^d = d(2\pi)^d / \mathcal{S}_d$, with $\mathcal{S}_d := 2\pi^{(d/2)} / \Gamma(d/2)$ the surface of the d -dimensional unit sphere. In $d = 2$ specifically, $\Lambda^2 = 4\pi$. In order to demonstrate that the fundamental frustration mechanism does not get lost due to the continuum approximation, we briefly rederive the canting threshold in Appendix B.

According to the scheme of the momentum-shell renormalization group, we now integrate out the spin modes with wave vectors in the shell $\Lambda e^{-d\ell} < k \leq \Lambda$. Thereby the original spin field \vec{S}^α is mapped onto the slowly varying background field \vec{s}^α . They are related by

$$\vec{S}^\alpha = \sqrt{1 - \chi_a^\alpha \chi_a^\alpha} \vec{s}^\alpha + \chi_a^\alpha \vec{e}_a^\alpha \quad (21)$$

with the vector fields \vec{e}_a^α forming a local orthonormal basis $\{\vec{e}_1^\alpha, \dots, \vec{e}_{N-1}^\alpha, \vec{s}^\alpha\}$ at each site \mathbf{r} in each replica α . We employ the sum convention for pairs of Latin indices ($a, b = 1, \dots, N-1$) only. The field χ_a^α generates an infinitesimal spin rotation and has contributions only from wave vectors in the momentum shell.

Derivatives of basis vectors can be expanded in the local bases

$$\partial_i \vec{s}^\alpha = B_{ia}^\alpha \vec{e}_a^\alpha, \quad (22a)$$

$$\partial_i \vec{e}_a^\alpha = -B_{ia}^\alpha \vec{s}^\alpha + A_{iab}^\alpha \vec{e}_b^\alpha \quad (22b)$$

in terms of potentials A and B . The arbitrariness of the choice of the vectors \vec{e}_a is reflected in a gauge invariance of the potentials; the gauge transformations are local rotations around \vec{s} .³³ One can exploit this gauge symmetry to show that the potential A corresponds to higher-order derivatives of the spin field.^{33,15} We ignore such contributions and therefore omit the potential A from now on.

For further calculations, χ can be considered as small since we consider an infinitesimal momentum shell. In addition, we treat temperature and disorder, which drive the fluctuations of χ , as small. In order to expand the Hamiltonian in χ , we first consider

$$\begin{aligned} \partial_i \vec{s}^\alpha &= B_{ia}^\alpha \vec{e}_a^\alpha - \chi_a^\alpha B_{ia}^\alpha \vec{s}^\alpha + \partial_i \chi_a^\alpha \vec{e}_a^\alpha - \chi_a^\alpha \partial_i \chi_a^\alpha \vec{s}^\alpha \\ &\quad - \frac{1}{2} \chi_b^\alpha \chi_b^\alpha B_{ia}^\alpha \vec{e}_a^\alpha + O(\chi^4) \end{aligned} \quad (23)$$

and, ordered by powers of χ ,

$$\psi_i = \psi_i^{(0)} + \psi_i^{(1)} + \psi_i^{(2')} + \psi_i^{(2'')} + O(\chi^3), \quad (24a)$$

$$\psi_i^{(0)} = \sum_\alpha B_{ia}^\alpha B_{ia}^\alpha = \sum_\alpha (\partial_i \vec{s}^\alpha)^2, \quad (24b)$$

$$\psi_i^{(1)} = \sum_\alpha 2 \partial_i \chi_a^\alpha B_{ia}^\alpha, \quad (24c)$$

$$\psi_i^{(2')} = \sum_\alpha \partial_i \chi_a^\alpha \partial_i \chi_a^\alpha, \quad (24d)$$

$$\psi_i^{(2'')} = \sum_\alpha \{ \chi_a^\alpha \chi_b^\alpha B_{ia}^\alpha B_{ib}^\alpha - \chi_b^\alpha \chi_b^\alpha B_{ia}^\alpha B_{ia}^\alpha \}. \quad (24e)$$

An expansion of the energy density for small χ gives

$$\begin{aligned} h(\psi_i) &= h(\psi_i^{(0)}) + h'(\psi_i^{(0)})[\psi_i^{(1)} + \psi_i^{(2')} + \psi_i^{(2'')} \\ &\quad + \frac{1}{2} h''(\psi_i^{(0)})[\psi_i^{(1)}]^2 + O(\chi^3). \end{aligned} \quad (25)$$

Substituting this expression back into Eq. (20), we rewrite

$$\mathcal{H} = \mathcal{H}_{\text{free}} + \mathcal{H}_{\text{int}}, \quad (26a)$$

$$\mathcal{H}_{\text{free}} = \int d^d r \sum_i \left\{ \frac{1}{2} K_l [\psi_i^{(0)} + \psi_i^{(2')}] - R_l(\psi_i^{(0)}) \right\}, \quad (26b)$$

$$\begin{aligned} \mathcal{H}_{\text{int}} &= \int d^d r \sum_i \left\{ \frac{1}{2} K_l [\psi_i^{(1)} + \psi_i^{(2'')}] - R_l'(\psi_i^{(0)}) \right. \\ &\quad \times [\psi_i^{(1)} + \psi_i^{(2')} + \psi_i^{(2'')}] - \frac{1}{2} R_l''(\psi_i^{(0)}) [\psi_i^{(1)}]^2 \left. \right\} \\ &\quad + O(\chi^3). \end{aligned} \quad (26c)$$

Hereby we have separated the “free” and “interaction” contributions in a way such that \mathcal{H}_{int} vanishes for $\chi=0$ and $\mathcal{H}_{\text{free}}$ contains the bilinear self-interaction of χ .

Due to the energy contribution \mathcal{H}_{int} the fluctuations cannot be integrated out exactly. In analogy to the treatment of the pure system, we apply standard perturbation theory to \mathcal{H}_{int} . In principle, this can be done in a systematic way at low temperatures, where $\chi \sim T^{1/2}$. Aiming at the analysis of the stability of magnetic order for low temperature and weak disorder, we retain only the renormalization effects to first order in \mathcal{H}_{int} . Integration over χ leads to an infinitesimal renormalization of the Hamiltonian

$$d\mathcal{H} = \langle \mathcal{H}_{\text{int}} \rangle + O(\mathcal{H}_{\text{int}}^2), \quad (27)$$

where the average is over the fluctuations of χ weighted by $\mathcal{H}_{\text{free}}$ only.

Using the averages

$$\langle \partial_i \chi_a^\alpha \partial_j \chi_b^\beta \rangle = \frac{1}{K_l} \delta_{ij} \delta_{ab} \delta^{\alpha\beta} dl, \quad (28a)$$

$$\langle \chi_a^\alpha \chi_b^\beta \rangle = \frac{d}{K_l \Lambda^2} \delta_{ab} \delta^{\alpha\beta} dl, \quad (28b)$$

one finds

$$\langle \psi_i^{(1)} \rangle = 0, \quad (29a)$$

$$\langle \psi_i^{(2')} \rangle = \frac{n}{K_l} dl, \quad (29b)$$

$$\langle \psi_i^{(2'')} \rangle = -(N-2) \frac{d}{K_l \Lambda^2} \psi_i^{(0)} dl, \quad (29c)$$

$$\langle [\psi_i^{(1)}]^2 \rangle = \frac{4}{K_l} \psi_i^{(0)} dl. \quad (29d)$$

Separating the flow of K_l and of R_l by the requirement $R_l'(0)=0$ as in Eqs. (19) for the bare quantities, we finally obtain the flow equations

$$\frac{d}{dl} K_l = (d-2)K_l - \frac{N-2}{\Lambda^2/d} - \frac{4}{K_l} R_l''(0), \quad (30a)$$

$$\begin{aligned} \frac{d}{dl} R_l(\psi) &= dR_l(\psi) - \left(2 + \frac{N-2}{K_l \Lambda^2/d} \right) \psi R_l'(\psi) \\ &\quad + \frac{2}{K_l} \psi [R_l''(\psi) - R_l''(0)]. \end{aligned} \quad (30b)$$

Terms explicitly proportional to the number of replicas n have been dropped. A rescaling $\mathbf{r} \rightarrow e^{dl} \mathbf{r}$ of lengths has been included in order to keep the value of the cutoff fixed.

For arbitrary temperature, the flow of K can be interpreted as a flow of the spin stiffness at fixed temperature. Using the dimensionless stiffness $j_l := K_l/K$, the dimensionless temperature $t := T/J = 1/K$, the rescaled field $\phi := \Delta K \psi$ (we recall that K and Δ are unrenormalized quantities), and $\hat{R}_l(\phi) := R_l(\psi)$, we rewrite the flow equations as

$$\frac{d}{dl} j_l = (d-2)j_l - \frac{N-2}{\Lambda^2/d} t - \frac{4\Delta^2}{j_l} \hat{R}_l''(0), \quad (31a)$$

$$\begin{aligned} \frac{d}{dl} \hat{R}_l(\phi) &= d\hat{R}_l(\phi) - \left(2 + \frac{N-2}{\Lambda^2/d} \frac{t}{j_l} \right) \phi \hat{R}_l'(\phi) \\ &\quad + \frac{2\Delta}{j_l} \phi [\hat{R}_l''(\phi) - \hat{R}_l''(0)]. \end{aligned} \quad (31b)$$

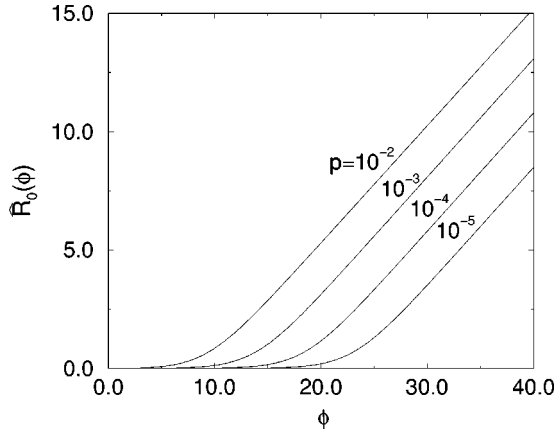


FIG. 1. Plot of the initial function $\hat{R}_0(\phi)$ for the values $p = 10^{-2}$, 10^{-3} , 10^{-4} , and 10^{-5} . Note that this nonanalytic function is very small up to $\phi^* = 2 \ln(1-p)/p$, where it assumes a slope that is approximately independent of small p .

In this form, temperature and disorder strength Δ appear as explicit parameters. The flow Eqs. (31) have to be solved with the initial conditions

$$j_0 = 1 - p\Delta, \quad (32a)$$

$$\hat{R}_0(\phi) = \ln[1 - p + pe^{\phi/2}] - \frac{1}{2}p\phi. \quad (32b)$$

Corresponding to the neglect of higher-orders of \mathcal{H}_{int} in Eq. (27), these flow equations contain renormalization effects only to the leading order in temperature and disorder. Higher orders of perturbation theory would certainly generate higher order contributions as well as a more complicated functional form of the Hamiltonian. Anticipating that $\hat{R}_l''(0) \geq 0$ is preserved under the flow, Eq. (31a) shows that both thermal fluctuations and disorder tend to reduce the effective stiffness.

In the given order, several features of the flow equations are remarkable. The initial function $\hat{R}_0(\phi)$ depends only on p (see Fig. 1). The crossover from the linear regime at small ϕ to the linear regime at large ϕ occurs at $\phi^* = 2 \ln(1-p)/p$, where the curvature $\hat{R}_0''(\phi) = 1/16 \cosh^2[(\phi - \phi^*)/4]$ has its maximum $\hat{R}_0''(\phi^*) = 1/16$. The flow equation of the stiffness couples to disorder only through $\hat{R}_0''(0)$. For $\Delta = 0$, this coupling vanishes, while $\hat{R}_l(\phi) = 0$ for $p = 0$. The flow equations depend on N only at finite temperatures (unlike the flow equations of Ref. 15). Thus, the properties at zero temperature are expected to be independent of N . However, one has to keep in mind that the equations apply only to spins with a continuous rotation symmetry ($N \geq 2$) and that the renormalization scheme ignores the effects of topological defects, which are known to be particularly important for $N = 2$.

IV. RESULTS AND DISCUSSION

In order to determine the large-scale properties of the model, we numerically integrate the coupled flow Eqs. (31)

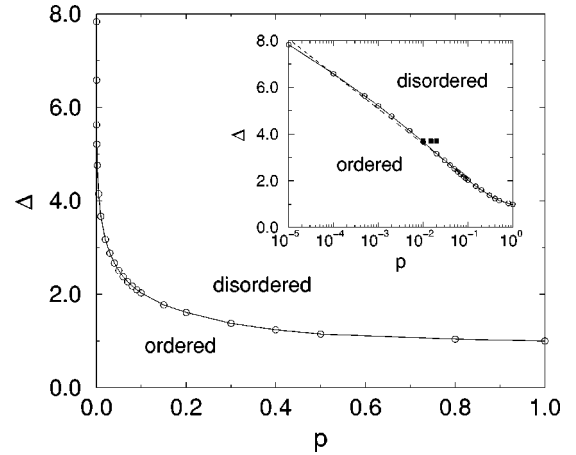


FIG. 2. Two-dimensional phase diagram at $T=0$ in a linear and semilogarithmic plot. The solid line represents the transition line $\Delta_{\text{FM}}(p)$ from the magnetically ordered to the disordered phase. In the inset the dashed line represents the linear fit (35) and the three filled squares represent the points with $\Delta = 3.7$ with $p = 0.01$, 0.015 , and 0.02 used in Sec. IV C for comparison with experiments.

for j_l and $\hat{R}_l(\phi)$ from $l=0$ to large l . If j_l converges for $l \rightarrow \infty$ to a finite value much larger than t , the system is in an ordered state with finite renormalized stiffness and infinite correlation length, i.e., $\langle \vec{S}(\mathbf{r}) \vec{S}(\mathbf{r}') \rangle = \lim_{n \rightarrow 0} \langle \vec{S}^\alpha(\mathbf{r}) \vec{S}^\alpha(\mathbf{r}') \rangle$ decays more slowly than exponentially with the distance $|\mathbf{r} - \mathbf{r}'|$. If, on the other hand, j_l becomes of order t on a finite scale $l = l^*$, the system is disordered and we identify the correlation length as

$$\xi = A e^{l^*} \quad (33)$$

with some constant A of the order of the lattice spacing. Following previous references,^{4,15} we specifically define this scale from

$$j_{l^*} = \frac{t}{2\pi}. \quad (34)$$

The influence of disorder in determining the correlation length is twofold: the starting value j_0 , Eq. (32a), depends explicitly on the disorder parameters, and the disorder contribution in Eq. (31a) leads to a faster decrease of j_l .

The critical disorder strength Δ_{FM} separating a ferromagnetically ordered phase from a disordered phase can be identified with the line where ξ diverges. Unfortunately, this criterion does not allow for a distinction between true long-range order and quasi-long-range order in the ferromagnetic phase.

A. Zero temperature

At $T=0$, we find the transition line $\Delta_{\text{FM}}(p)$ as shown in Fig. 2. This transition has the following features.

1. Regime of small p

For dilute disorder, $p \rightarrow 0$, we find a slow but unbounded increase of $\Delta_{\text{FM}}(p)$. In the range $10^{-5} \leq p \leq 0.1$ the line follows roughly the relation (see the dashed line in the inset of Fig. 2)

$$\Delta_{\text{FM}}(p) \approx 0.606 + 0.648 \ln \frac{1}{p}. \quad (35)$$

However, in the limit $p \rightarrow 0$, $\Delta_{\text{FM}}(p)$ appears to increase more slowly than logarithmically.

This finding implies order below a finite defect concentration even for arbitrarily strong defect bonds. This behavior is in disagreement with Refs. 14 and 15, where disorder (with $\Delta > \Delta_{\text{single}}$) was suggested to destroy order for infinitesimally small p . As already stated in Sec. II D, we believe that the effects of disorder are overestimated in both previous approaches because of special assumptions about the nature of the bivectorial field \vec{f}_i .

For the special case $N=2$, where this disagreement persists, further references can be included in the comparison. (We assume here that XY and Heisenberg systems should have a similar phase diagram at $T=0$ since our lowest-order flow equations are independent of N . Topological defects are ignored in our work as well as in Ref. 15. Their presence may further reduce ξ .) Although the XY model with random-phase shifts is *a priori* a different model, the effect of disorder is represented by a random distribution of dipoles such as that in model (1).³⁴ Various recent work (see, e.g., Refs. 25 and 35) has provided evidence that quasi-long-range order exists for weak disorder (even in the presence of vortices). This observation is consistent with our flow equations but contradicts the flow equations of Cherepanov *et al.*¹⁵ From their numerical data, Gawiec and Gempel²³ argue for a disordered phase for $\Delta > \Delta_{\text{single}}$ and $p > 0$, i.e., for $\Delta_{\text{FM}}(0) = 2$. While this conclusion is again in disagreement with our result, the numerical data are not: Gawiec and Gempel²³ present data for $\Delta = 4$ as the only value with $\Delta > 2$ and they demonstrate the absence of order only for $p \geq 0.02$. For $\Delta = 4$, we find order at very small $p \leq 0.0062$, which actually is *not* excluded by the numerical data (cf. Fig. 17 of Ref. 23).

2. Regime of large p

For $p \rightarrow 1^-$ we find that $\Delta_{\text{FM}}(p) \rightarrow 1^+$ in a smooth way. While this is qualitatively correct, a horizontal segment with $\Delta_{\text{FM}}(p) = 1$ beyond the percolation transition at $p = \frac{1}{2}$ is absent. However, in this range we find $\Delta_{\text{FM}}(p)$ which is only slightly larger, i.e., this is a quantitative effect which may be attributed to the continuum approximation as argued in the text below Eq. (20). In addition, the regime near $\Delta = 1$ and $p \gtrsim \frac{1}{2}$ is a regime of strong disorder in the sense of the content of Sec. II C since $\sigma^2 \gtrsim 1$. There our flow equations are not quantitatively reliable because of the lowest-order truncation. On the other hand, the transition at small p should be well described since Eq. (9) is satisfied, $p\Delta_{\text{FM}}^2(p) \rightarrow 0$ for $p \rightarrow 0$.

When the transition line is approached at finite p , the correlation length displays a divergence,

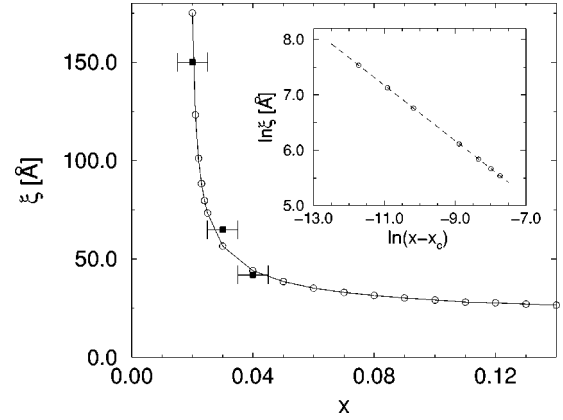


FIG. 3. Plot of $\xi(x)$ for $T=0$ with $\Delta=3.7$ and $A=22 \text{ \AA}$ in order to fit the experimental data (filled squares with error bars) of Ref. 36. The inset shows a double-logarithmic plot of ξ as a function of $x-x_c$ for $\Delta=3.7$ with $x_c=0.019 062$. Open circles connected by a line represent ξ calculated numerically from the flow equations. The dashed line is the best linear fit with slope $-\nu = -0.500 07$.

$$\xi(\Delta, p) \sim [\Delta - \Delta_{\text{FM}}(p)]^{-\nu}. \quad (36)$$

From the numerical integration of our flow equations we find a mean-field-like exponent $\nu=0.500(1)$ (see the inset of Fig. 3). The finding of the mean-field value is probably related to the neglect of higher-order terms in our flow Eqs. (31).

B. Finite temperatures

Temperature enters the flow equations in two places where it could lead to contrary effects. In Eq. (31a), an increase of temperature leads to a faster renormalization of the spin stiffness to smaller values [ignoring the temperature dependence of $\hat{R}'_l(0)$]. On the other hand, in Eq. (31b) temperature tends to suppress \hat{R} , which might in turn reduce the efficiency of disorder in suppressing the spin stiffness. However, from our flow equations, we always find that thermal fluctuations reduce stiffness and therefore also ξ .

More precisely, ξ decreases monotonously with increasing temperature. Thus, a reentrant temperature dependence as found by GI (Ref. 14) is absent in the present treatment. We attribute this discrepancy to the fact that GI kept the length of the bivector \vec{f}_i fixed, whereas its typical length should vanish at low T according to Eq. (12). Thereby, with decreasing temperature, the strength of disorder is increasingly overestimated, giving way to an apparent reentrance.

C. Comparison with experiments

We now turn to check the consistency of our theory with measurements on $\text{La}_{2-x}\text{Sr}_x\text{CuO}_4$. To allow for a comparison of our results with those of Cherepanov *et al.*¹⁵ we refer to the same experimental data of Keimer *et al.*³⁶ for $x=0.02, 0.03, \text{ and } 0.04$. For the moment we assume that interlayer couplings and spin anisotropies can be neglected and we will come back to this issue later.

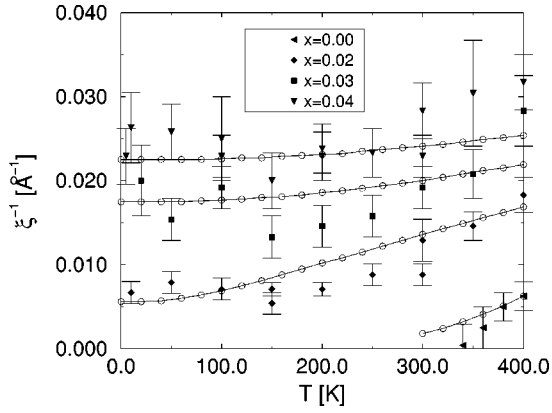


FIG. 4. Plot of $\xi^{-1}(T)$ for $x=0, 0.02, 0.03,$ and 0.04 . Symbols with error bars are experimental data from Ref. 36. Open circles connected by lines represent our theory.

The comparison of our results for ξ with experiments involves four parameters, $p, \Delta, J,$ and A . As already stated above, our model parameter $p=x/2$ is directly related to the dopant concentration x . A is a length scale of the order of the lattice spacing. In principle, this parameter can depend on temperature and disorder itself (see the discussion in Ref. 15). Such dependencies could modify the function $\xi(x, T)$ in a subdominant way and would involve additional assumptions and parameters. We refrain from including such dependencies for the purpose of the subsequent semiquantitative comparison.

At $T=0$, J does not enter the flow equations since it simply sets the energy scale and Δ is the only unknown model parameter which enters the numerical calculation of l^* . From the consideration of the superexchange across a defect bond, one expects $\Delta \gg 1$,⁶ i.e., a value clearly above the canting instability. The finiteness of the measured values of ξ for $x \geq 0.02$ implies that the data points lie in the disordered phase, i.e., $\Delta > \Delta_{\text{FM}}(p=0.01) \approx 3.67$.

We have determined values of the parameters $\Delta, A,$ and J from the requirement that our theoretical values for ξ should be consistent with experimental data. In view of the given experimental errors and the approximate nature of our RG calculation, we found a satisfactory agreement for

$$\Delta = 3.7, \quad (37a)$$

$$J = 240 \text{ K}, \quad (37b)$$

$$A = 5.8a, \quad (37c)$$

where $a = 3.8 \text{ \AA}$ is the lattice spacing. In Fig. 3 we compare our theory with data for ξ as a function of x at $T=0$. The inset shows for $\Delta = 3.7$ a double-logarithmic plot of $\xi(x)$ which reveals the mean-field-like divergence of ξ according to Eq. (36) near the order-disorder transition.

The temperature dependence of ξ is shown in Fig. 4. Keeping in mind the strong fluctuations of the experimental data, they can be considered as consistent with our analysis. However, the theoretical dependence of ξ on T and p does not quantitatively confirm the empirical formula^{2,36}

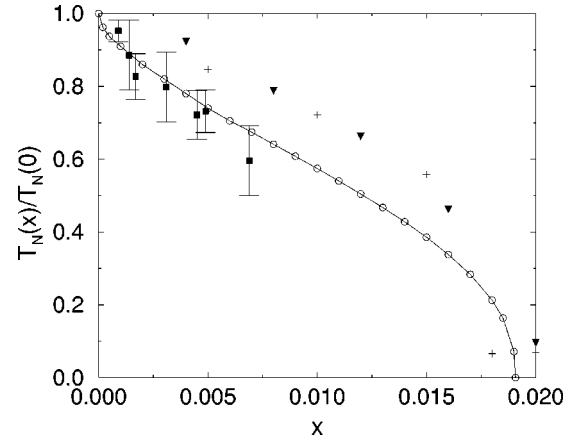


FIG. 5. Plot of our numerical result for $T_N(x)$ (open circles connected by a line). For comparison, squares (Ref. 39), triangles (Ref. 40), and crosses (Ref. 41) represent experimental data (see the main text).

$$\xi^{-1}(T, p) = \xi^{-1}(T, 0) + \xi^{-1}(0, p), \quad (38)$$

which would imply that in Fig. 4 the curves for different p should differ only by a vertical shift. In contrast, we find that thermal fluctuations lead to a stronger increase of ξ^{-1} for smaller p .

In comparing experimental data to the results from our model one may wonder whether the exchange couplings can be considered as quenched at higher temperatures. Indeed, holes are no longer localized but have a thermally activated mobility characteristic of variable-range hopping which is very small up to temperatures near 50 K.³⁷ However, in order to have quenched exchange couplings it is not necessary to have strictly localized holes. To obtain dipolar spin textures (at least on a coarse-grained length scale) it is sufficient to have a sufficiently inhomogeneous density distribution.¹⁵

D. Coupled layers

We now address the effects of a very weak interlayer coupling J^\perp . For La_2CuO_4 , a ratio $J^\perp/J = 5 \times 10^{-5}$ was determined from experiments.⁵ From a simple scaling analysis,³⁸ one immediately obtains the flow equation

$$\frac{d}{dl} J_i^\perp = 2J_i^\perp, \quad (39)$$

which shows the strong relevance of this coupling. From the condition that the interlayer coupling becomes comparable to the intralayer coupling, $J_i^\perp = J$, one can fix a dimensional crossover scale

$$\ell^\perp = \frac{1}{2} \ln \frac{J}{J^\perp}. \quad (40)$$

Comparing this scale with the correlation length (33) obtained in the *absence* of the layer coupling, one expects that the coupling actually is irrelevant for $l^* < \ell^\perp$, where 2D fluctuations on small scales renormalize J^\perp to zero. On the other hand, for $l^* > \ell^\perp$, fluctuations become three dimen-

sional on scales larger than ℓ^\perp . Per the definition of l^* , the exchange coupling on the scale ℓ^\perp is still large compared to temperature such that magnetic long-range order should be stable. Therefore, the location of three-dimensional ordering in the (x, T) plane can be determined from the implicit condition

$$l^*(x, T) = \frac{1}{2} \ln \frac{J}{J^\perp}. \quad (41)$$

We have evaluated this condition numerically for $J^\perp/J = 5 \times 10^{-5}$ and the parameter set (37). The resulting Néel temperature is plotted in Fig. 5 as a function of doping. The transition temperature is normalized by its value $T_N(0) \approx 300$ K in the absence of disorder, which essentially reflects the value of J . While the precise value of J may vary to some extent with the employed fitting procedure for the parameter set, the shape of the normalized transition line is very robust. At $T=0$, the critical disorder strength x_{3D} is increased by the interlayer coupling only slightly over $x_{2D} \approx 0.1906$, $(x_{3D} - x_{2D})/x_{2D} \approx 10^{-2}$, because of the extremely slow divergence of ξ for $x \rightarrow x_{2D}^+$.

In comparison to the theory in Ref. 15, we find that $T_N(x)$ decays less abruptly near x_{3D} . We compare our results to data from Hall measurements³⁹ (squares in Fig. 5), susceptibility measurements⁴⁰ (triangles), and perturbed angular correlation measurements⁴¹ (crosses). The overall agreement is satisfying, although the experimental data partially suggest that disorder is less effective in reducing the transition temperature. This tendency may be attributed to the fact that the samples were partially oxygen doped (at higher temperature, oxygen is not quenched and is less effective in generating spin frustration) as well as the fact that we have neglected the easy-plane spin anisotropy, which also tends to stabilize the magnetic order.

While we have thus shown that a mechanism based on spin frustration by quenched disorder is consistent with the experimental data, completely different mechanisms (for example, nonlinear- σ models with effective, doping dependent exchange constants^{42,43}) have been suggested in the past which also lead to qualitatively similar phase diagrams. Furthermore, the assumption of a site dilution by holes can lead to a similar phase diagram.⁴⁴ In order to discriminate between the different models it would be desirable to have experimental data from which one can decide whether the spin-correlation function at low temperatures has true long-range order (this would be consistent with a homogeneous spin system with effective spin stiffness) or whether it has only quasi-long-range order (this would be consistent with the frustration mechanism).

V. CONCLUSIONS

In this paper, we have reexamined a classical model for N -component spins ($N \geq 2$) with random exchange couplings and we have chosen an approach complementary to previous studies by Glazman and Iosevich¹⁴ and Cherepanov *et al.*¹⁵ Special care has been taken to preserve the quenched nature of disorder and the global spin rotation symmetry.

Our analysis involves approximations which we briefly summarize. (i) The originally discrete spin system is represented in a continuum formulation. Thus, features related to the specific lattice structure—such as the location of the percolation transition for $\Delta = 1$ —cannot be captured quantitatively. (ii) As in the pure case, the renormalization scheme accounts only for interactions between spin waves, ignoring the role of topological defects. Thus, the degree of magnetic order may be overestimated (recall that for $N=2$ the pure system erroneously appears to be ordered at all temperatures if vortices are neglected). (iii) The flow equations are truncated to lowest order in temperature and disorder. In principle, the analysis could be extended to higher orders. In practice, this extension is hampered by a much more complicated functional form of the Hamiltonian which is generated during the flow.

Due to the nonanalytic nature of the cumulant function R , we found it necessary to develop a *functional* renormalization group, i.e., to keep track of *arbitrarily high cumulants* of the disorder distribution. To the best of our knowledge, functional flow equations for disordered spin systems have been considered previously only for different types of disorder, in particular for random fields and random anisotropy.^{45–48}

The flow Eqs. (31) are the central result of the analytic part of this work. For comparison, the analysis of Cherepanov *et al.*,¹⁵ which employs approximations corresponding to the ones listed above, is restricted to a single disorder parameter that corresponds to the lowest cumulant of the disorder distribution.

As a main physical result of our RG analysis, we find that the two-dimensional spin system can be magnetically ordered at $T=0$ in the presence of a sufficiently small but *finite* concentration of arbitrarily strong defects ($\Delta > \Delta_{\text{single}}$). At this point it is worthwhile to recall that we have identified magnetic order from the length scale where the spin stiffness is renormalized down to the scale of thermal fluctuations. In the absence of explicit calculations for the spin-spin correlation function it is natural to assume that this scale coincides with the magnetic correlation length ξ . Such a calculation would be desirable in order to clarify whether the ordered phase (with $\xi = \infty$) has quasi-long-range order or true long-range order. We have determined ξ by a numerical integration of our flow equations for the strictly two-dimensional system as well as for weakly coupled layers. In the first case our zero-temperature phase diagram is consistent with numerical simulations.²³ In the second case, the calculated dependence of ξ on temperature and disorder strength is in good agreement with measurements on cuprates. In both cases the comparison was restricted to *finite* length scales given by the computationally manageable system sizes or the experimental error bars, respectively.

Nevertheless, concerning the question of whether magnetic order is stable against bond disorder in two dimensions on largest scales, our positive answer, shared by Ref. 16, disagrees with previous negative ones.^{14,15} In the end of Sec. II D we have given specific reasons why in our opinion the previous answers cannot be considered as final. In view of the complementary approaches and approximations involved, this question has to be considered as an open one that calls for additional research.

ACKNOWLEDGMENTS

We gratefully acknowledge discussions with A. Aharony, D. R. Grempel, T. Nattermann, H. Rieger, and B. Rosenow.

APPENDIX A: DUALITY

For the bimodal distribution (3) with $\Delta > 1$, our system consists of a fraction p of “defective” antiferromagnetic bonds and a fraction $1 - p$ of “regular” ferromagnetic bonds. The relative strength of bonds is $|J_{\text{AFM}}/J_{\text{FM}}| = 1 - \Delta$. From a dual point of view, one may say that the system consists of a fraction $\tilde{p} := 1 - p$ of “defective” ferromagnetic bonds and a fraction $1 - \tilde{p} = p$ of “regular” antiferromagnetic bonds. Since for classical spins thermodynamic properties are invariant under flipping one sublattice and reversing the sign of the exchange coupling ($J_{\text{AFM}} = -\tilde{J}_{\text{FM}}$ and $J_{\text{FM}} = -\tilde{J}_{\text{AFM}}$),¹⁹ the system is equivalent to a system with a fraction $\tilde{p} := 1 - p$ of “defective” antiferromagnetic bonds and a fraction $1 - \tilde{p} = p$ of “regular” ferromagnetic bonds of relative strength $|\tilde{J}_{\text{AFM}}/\tilde{J}_{\text{FM}}| = 1/(1 - \Delta) =: 1 - \tilde{\Delta}$.²⁷ Thus duality provides a mapping,

$$J \rightarrow \tilde{J} = (1 - \Delta)J, \quad (\text{A1a})$$

$$p \rightarrow \tilde{p} = 1 - p, \quad (\text{A1b})$$

$$\Delta \rightarrow \tilde{\Delta} = \frac{\Delta}{\Delta - 1}, \quad (\text{A1c})$$

for all temperatures.

APPENDIX B: CONTINUUM LIMIT

We show that the spin frustration mechanism is well captured in the continuum representation of our model. To this

end, we rederive the canting instability threshold $\Delta_{\text{single}} = d$ for a single defect bond. For a single defect bond located at $\mathbf{r} = \mathbf{0}$ and oriented in direction \mathbf{e}_j the Hamiltonian reads

$$H = \frac{J}{2} \int d^d r \sum_i [1 - \delta_{ij} \delta(\mathbf{r}) \Delta] [\partial_i \vec{S}(\mathbf{r})]^2. \quad (\text{B1})$$

We introduce a canting field $\vec{\chi}(\mathbf{r})$, $\vec{\chi}^2(\mathbf{r}) \leq 1$, perpendicular to a collinear ground state $\vec{S}_0(\mathbf{r}) \equiv \vec{S}_0$ of the pure system via

$$\vec{S}(\mathbf{r}) = \sqrt{1 - \vec{\chi}^2(\mathbf{r})} \vec{S}_0 + \vec{\chi}(\mathbf{r}). \quad (\text{B2})$$

To show the canting instability we insert Eq. (B2) into the Hamiltonian and minimize the energy with respect to the canting field $\vec{\chi}$ after expanding the Hamiltonian up to quadratic order in this field. In Fourier space the saddle-point equation reads

$$\vec{\chi}_{\mathbf{q}} = \Delta \frac{q_j}{q^2} \int_{\mathbf{k}} k_j \vec{\chi}_{\mathbf{k}}. \quad (\text{B3})$$

Multiplying Eq. (B3) with q_i and integrating over \mathbf{q} we get

$$\vec{\mu}_i = \frac{\Delta}{d} \delta_{ij} \vec{\mu}_j, \quad (\text{B4})$$

with

$$\vec{\mu}_i := \int_{\mathbf{k}} k_i \vec{\chi}_{\mathbf{k}}. \quad (\text{B5})$$

This self-consistency condition on $\vec{\mu}_i$ implies

$$\Delta = \Delta_{\text{single}} = d \quad (\text{B6})$$

for a nonvanishing solution of the saddle-point equation (B3).

¹K. Binder and A. P. Young, Rev. Mod. Phys. **58**, 801 (1986).

²G. Shirane, R. J. Birgeneau, U. Endoh, and M. A. Kastner, Physica B **197**, 158 (1994).

³We refer to the square lattice only in a topological sense, not in the strict geometric sense. The materials of interest may exist in tetragonal and in orthorhombic phases. In the latter the squares are deformed leading to a reduced symmetry. We neglect a possible anisotropy in the exchange couplings as well as couplings between more distant spins.

⁴S. Chakravarty, B. I. Halperin, and D. R. Nelson, Phys. Rev. B **39**, 2344 (1989).

⁵B. Keimer, A. Aharony, A. Auerbach, R. J. Birgeneau, A. Casanholo, Y. Endoh, R. W. Erwin, M. A. Kastner, and G. Shirane, Phys. Rev. B **45**, 7430 (1992).

⁶A. Aharony, R. J. Birgeneau, A. Coniglio, M. A. Kastner, and H. E. Stanley, Phys. Rev. Lett. **60**, 1330 (1988).

⁷R. J. Gooding and A. Mailhot, Phys. Rev. B **44**, 11 852 (1991).

⁸H. J. Schulz, J. Phys. (France) **50**, 2833 (1989).

⁹J. Zaanen and O. Gunnarsson, Phys. Rev. B **40**, 7391 (1989).

¹⁰V. J. Emery and S. A. Kivelson, Physica C **209**, 597 (1993).

¹¹F. C. Chou, N. R. Belk, M. A. Kastner, R. J. Birgeneau, and A. Aharony, Phys. Rev. Lett. **75**, 2204 (1995).

¹²A. M. Polyakov, Phys. Lett. **59B**, 79 (1975).

¹³J. Villain, Z. Phys. B **33**, 31 (1979).

¹⁴L. I. Glazman and A. S. Ioselevich, Z. Phys. B: Condens. Matter **80**, 133 (1990).

¹⁵V. Cherepanov, I. Y. Korenblit, A. Aharony, and O. Entin-Wohlman, Eur. Phys. J. B **8**, 511 (1999).

¹⁶J. P. Rodriguez, J. Bonca, and J. Ferrer, Phys. Rev. B **51**, 3616 (1995).

¹⁷V. J. Emery and G. Reiter, Phys. Rev. B **38**, 4547 (1988).

¹⁸For anisotropic bond-disordered spin systems this assumption is supported by a $1/S$ expansion for the phases with long-range order [P. Gawiec and D. R. Grempel, Phys. Rev. B **54**, 3343 (1996)].

¹⁹E. Fradkin, B. A. Huberman, and S. H. Shenker, Phys. Rev. B **18**, 4789 (1978).

²⁰J. Villain, J. Phys. C **10**, 4793 (1977).

- ²¹J. Villain, *J. Phys. (France)* **38**, 385 (1977).
- ²²W. M. Saslow and G. N. Parker, *Phys. Rev. B* **38**, 11 733 (1988).
- ²³P. Gawieć and D. R. Grempel, *Phys. Rev. B* **44**, 2613 (1991).
- ²⁴G. N. Parker and W. M. Saslow, *Phys. Rev. B* **38**, 11 718 (1988).
- ²⁵T. Nattermann, S. Scheidl, S. E. Korshunov, and M. S. Li, *J. Phys. I* **5**, 565 (1995).
- ²⁶C. Timm and K. H. Bennemann, *Phys. Rev. Lett.* **84**, 4994 (2000).
- ²⁷P. Gawieć and D. R. Grempel, *Phys. Rev. B* **48**, 7114 (1993).
- ²⁸M. F. Sykes and J. W. Essam, *J. Math. Phys.* **5**, 1117 (1964).
- ²⁹J. Vannimenus, S. Kirkpatrick, F. D. M. Haldane, and C. Jayaprakash, *Phys. Rev. B* **39**, 4634 (1989).
- ³⁰See also the related discussion in Ref. 23.
- ³¹Y. Nonomura and Y. Ozeki, *J. Phys. Soc. Jpn.* **64**, 2710 (1995).
- ³²N. D. Mermin and H. Wagner, *Phys. Rev. Lett.* **17**, 1133 (1966).
- ³³A. M. Polyakov, *Gauge Fields and Strings* (Harwood, Academic, Sutherland, Chur, 1987).
- ³⁴M. Rubinstein, B. Shraiman, and D. R. Nelson, *Phys. Rev. B* **27**, 1800 (1983).
- ³⁵S. Scheidl, *Phys. Rev. B* **55**, 457 (1997).
- ³⁶B. Keimer, N. Belk, R. J. Birgeneau, A. Cassanho, C. Y. Chen, M. Greven, M. A. Kastner, A. Aharony, Y. Endoh, R. W. Erwin, and G. Shirane, *Phys. Rev. B* **46**, 14 034 (1992).
- ³⁷M. A. Kastner, R. J. Birgeneau, C. Y. Chen, Y. M. Chiang, D. R. Gabbe, H. P. Jenssen, T. Junk, C. J. Peters, P. J. Picone, T. Thio, T. R. Thurston, and H. L. Tuller, *Phys. Rev. B* **37**, 111 (1988).
- ³⁸J. M. Kosterlitz and D. J. Thouless, in *Progress in Low Temperature Physics*, edited by D. F. Brewer (North-Holland, Amsterdam, 1978), Vol. VII B.
- ³⁹C. Y. Chen, R. J. Birgeneau, M. A. Kastner, N. W. Preyer, and T. Thio, *Phys. Rev. B* **43**, 392 (1991).
- ⁴⁰J. H. Cho, F. C. Chou, and D. C. Johnston, *Phys. Rev. Lett.* **70**, 222 (1993).
- ⁴¹J. Saylor and C. Hohenemser, *Phys. Rev. Lett.* **65**, 1824 (1990).
- ⁴²A. H. Castro Neto and D. Hone, *Phys. Rev. Lett.* **76**, 2165 (1996).
- ⁴³E. C. Marino and M. B. Silva Neto, *Phys. Rev. B* **64**, 092511 (2001).
- ⁴⁴Y.-C. Chen and A. H. Castro Neto, *Phys. Rev. B* **61**, R3772 (2000).
- ⁴⁵D. S. Fisher, *Phys. Rev. B* **31**, 7233 (1985).
- ⁴⁶D. E. Feldman, *Pis'ma Zh. Éksp. Teor. Fiz.* **70**, 130 (1999) [*JETP Lett.* **70**, 135 (1999)].
- ⁴⁷D. E. Feldman, *Phys. Rev. B* **61**, 382 (2000).
- ⁴⁸D. E. Feldman, *Phys. Rev. Lett.* **88**, 177202 (2002).